



Soil nematode fauna in rice paddy fields from Taiwan based on morphology and DNA barcoding

Ming-Chung CHIU^{1,2,3}, Tang-Wei LIN^{1,4}, Zhao-Hui LIN^{1,4}, Li-Yen LEE¹, Po-Wei HSU², Hsuan-Wien CHEN^{1*}

1. Department of Biological Resources, National Chiayi University, Chiayi 600, Taiwan. 2. Department of Biology, National Changhua University of Education, Changhua 500, Taiwan. 3. Department of Entomology, National Taiwan University, Taipei 106, Taiwan. 4. Endemic Species Research Institute, Council of Agriculture, Nantou, 552, Taiwan. *Corresponding authors' emails: chen7@mail.ncyu.edu.tw

(Manuscript received 25 April 2024; Accepted 1 September 2024; Online published 6 September 2024)

ABSTRACT: Nematodes adapt to variety of environments. Dynamics of a nematode community are highly associated with the soil condition, which can serve as an indicator for monitoring the impact of human activity on the soil ecosystem. However, a systematic study on nematode fauna is lacking in many regions across Taiwan. In this study, we provide morphological and molecular identification for the soil nematodes collected during the cultivation process of the first crop rice in Chiayi, Taiwan. Within the three-year survey, 26 morphospecies of 18 genera were identified in the soil from the rice paddy fields. Each morphospecies was initially identified based on morphology, and 11 were further examined using 18S rDNA sequences. Among these, nine predominant morphospecies represented over 90% of the abundance, while juveniles of the plant pathogenetic nematode, *Meloidogyne*, were the most abundant one. Bacterivore was the most diverse and abundant functional group in the nematode community. Eight morphospecies were supported by the molecular identification at the genus level, while three require further consideration due to inconsistencies between morphological and molecular analyses.

KEY WORDS: free-living nematode, functional group, molecular identification, morphological description, rice paddy field.

INTRODUCTION

Nematodes are diverse animals that adapt to various environments (Chen *et al.*, 2014). Depending on their parasitic characteristics, many of them are tightly associated with human life, including public health (e.g., Grove, 1990), plant diseases (e.g., Jatala, 1986), and pest management (e.g., Kaya and Gaugler, 1993). However, free-living nematodes, accounting for the majority of nematode fauna, are often overlooked. In agricultural systems, crop health is not only impacted directly by plant-pathogenic or entomopathogenic nematodes (Kanwar *et al.*, 2021), but also by those with diverged feeding habits in soil which occupy different niches and trophic levels (Yeates *et al.*, 1993). These soil nematodes possess significant ecosystem functions, evident from the fact that they are usually composed by phylogenetically distinct nematode lineages. The presence of diverse soil nematodes can promote mineralization (Ferris *et al.*, 1998; Chen and Ferris, 1999), inhibit populations of plant-pathogenic nematodes (Steel and Ferris, 2016), and accelerate plant growth and its nutrition intake (Gebremikael *et al.*, 2016). Given their various ecological functions, soil nematode communities have also been widely used as bio-indicator for soil conditions. It started with the use of abundance of a single species in 1970s and has evolved to include a combination of multiple parameters regarding species diversity, trait-based index (Neher, 2001), life history, and functional group (Bongers, 1990; Ferris *et al.*, 2001), and body size (Andriuzzi and

Wall, 2018). To date, the method has been widely adopted in various agriculture systems to assess soil condition and assist farmers in decision-making, including evaluating the effects of fertilizer (Chen *et al.*, 2014), agricultural practices (Zhang *et al.*, 2015), organic farming (Sánchez-Moreno *et al.*, 2018), and clear-cut in artificial forests (George and Lindo, 2015).

It is estimated that no more than 10% of total nematode species have been described, and nematode fauna in many areas has never been investigated (Ahmed *et al.*, 2015). Highlighting the importance of a 'nematode indicator' for monitoring environmental changes, De Ley (2000) suggested a greater focus on taxa with ecological, economic, and medical significance, focusing on resolving major pattern of nematode community and functional associations between communities rather than solely describing species. Pioneer studies on the free-living soil nematodes in Taiwan have been conducted in 2011–2013. The list of the nematode genera made by morphological identification served as one of the important information for the soil nematode fauna for the forests and agriculture systems in Taiwan (Ho, 2011; Liao, 2012; Jhao, 2013). However, integration of morphological with molecular data was still lacking to date. Rice (*Oryza sativa* L.), one of the three most important grain crops, is cultivated in a total of 160 million hectares of paddy fields worldwide (Watanabe, 2018). Cultivation of rice requires flooded fields, resulting in the creation of large-scale artificial and temporary wetland environments (Watanabe, 2018). This



unique landscape has its own ecosystem (Edirisinghe and Bambaradeniy, 2006) and is highly linked to the surrounding environment (Perret *et al.*, 2013) and climate change (de Miranda *et al.*, 2015; Min and Rulík, 2020). In the present study, we want to characterize species composition of the nematode community in rice paddy fields. Free-living nematodes were collected during a 3-year field survey in the rice fields, counted, and identified to genus level. This identification is sufficient to estimate the ecological function of the free-living nematode. Each morphospecies was photographed, and its morphology was described to facilitate future studies. In addition to the morphological description, molecular identification was included to assist our classification. Currently, DNA barcoding has been widely used for nematode identification. It is particularly helpful when nematode fauna description is not available. Therefore, predominant morphospecies in this study were selected for further DNA barcode sequencing and compared against those in the online database. We hope this study can serve as pioneering research not only in nematode taxonomy but also in rice field management in Taiwan.

MATERIAL AND METHODS

Soil sample collection

The study site was in the experimental rice paddy fields in Xikou experimental farm (23°34'56.1"N 120°24'16.0"E), Chiayi Agricultural Experimental Branch, Council of Agriculture, Executive Yuan, Taiwan. The soil at the sampling site was characterized as a non-calcareous sandy shale alluvial soil with a texture classified as silty clay loam. The pH of the soil at the sampling depth was measured at 6–7.5 (Chen *et al.*, 2009). Total size of the fields is around four hectares, comprising eight 50 × 100 m² separated fields.

The survey was conducted during the cultivation of the first crop rice (Late January to June) in 2018–2020, following the eight periods within the cultivation process, including soil loosening, flooding, transplanting, 1st topdressing (with application of herbicides mefenacet and butachlor), 2nd topdressing (with application of insecticides probenazole and cartap, as well as fungicide furametpyr), 3rd topdressing, field drying, harvesting. These collections covered five flooded periods (flooding, transplanting, 1st topdressing, 2nd topdressing, 3rd topdressing) and three drained periods (field drying, harvesting, soil loosening). Sample collections were conducted nine times in 2018 (twice after harvesting), seven times in 2019 (not collected after transplanting), and seven times in 2020 (not collected after soil loosening). For molecular identification, ten soil samples were collected during the 2nd topdressing in 2021.

Three rhizosphere soil samples, each collected approximately 5 cm from the base of the plants, were randomly obtained from within each of the eight 50 × 100

m² fields. Each sample was collected at least 20 m from the others and 1 meter away from the edge. In 2019 and 2020, each sample was made by pooling eight subsamples (no subsample was used in the collection in 2018), which are cylinders (5 cm in diameter and 10 cm depth) of soil collected from 3–15 cm depth. The soil is likely composed primarily of material from oxidized layers, as the deeper regions are densely packed and resemble clay. All the samples were transported to laboratory within three hours at room temperature.

Nematode extraction and preparation

Nematodes were extracted from approximate 400 g of moist soil sample using modified Baermann funnel method (Barker *et al.*, 1985). Briefly, soil was wrapped in tissue paper and placed onto a metal sieve (1 mm² mesh) set on a funnel. Opening of the funnel was equipped with a 13 mL collection bottle. The sample was immersed in 1000 mL of tap water (encompassing the entire setup from the collection bottle, funnel, to the sample) for 2 days to induce nematode precipitation into the collection bottle. Most of each sample was submerged in water, allowing nematodes to emerge not only from the bottom but also from various directions without being obstructed by clay soil that might block their entry into the water.

Morphological examination

Examination of nematodes referred to the modified method described in Ryss (2017). Nematodes in the suspension were killed by heating for 3–6 min at 90°C, photographed, and individually classified into morphospecies under a light microscope (Leica DM500, Wetzlar, Germany) at a magnification of 40–400×. For the detailed morphological description, nematodes treated with heat were first fixed by series of ethanol (50%, 75%, 90% ethanol) each for 15 minutes and finally in a 9:1 ethanol/glycerin mixture for overnight. Fixed nematodes were mounted on a glass slide with 2 mL ethanol/glycerin mixture, heated at 50°C until all ethanol had evaporated, and sealed under a cover slide using nail polish. Observation was conducted under an oil lens at a magnification of 1000×. The size of the nematodes was measured by photographing them using Image J (<https://imagej.net/ij/>).

Each of the morphospecies was identified to genus level according to the diagnostic keys provided by University of Nebraska-Lincoln (<https://nematode.unl.edu/nemakey.htm>), University of California, Davis (Nemaplex, <http://nemaplex.ucdavis.edu/Taxadata/Famkey.htm>), and Pictorial key to soil animals of China (Yin, 1992, 1998). Trophic levels (bacterivore, fungivore, herbivore, omnivore, predator) of each morphospecies and its *cp* values were classified according to the morphology of mouthpart and its taxonomic group (Yeates *et al.*, 1993; Bongers and Bongers, 1998; Ferris, 2010).

**Table 1.** Morphospecies of nematodes collected from the rice paddy field in Xikou.

Order	Family	morphospecies	cp	Functional group ²	Average abundance (nematode No. / 1g dry soil)			
					2018	2019	2020	Average (%)
Dorylaimida	Dorylaimidae	<i>Dorylaimus</i> sp1	4	omnivore	189.62	101.22	189.85	160.23 (12.26)
Dorylaimida	Dorylaimidae	<i>Dorylaimus</i> sp2	4	omnivore	11.05	1.70	1.28	4.67 (0.36)
Dorylaimida	Dorylaimidae	<i>Dorylaimus</i> sp3	4	omnivore	1.10	0.00	0.00	0.37 (0.03)
Dorylaimida	Dorylaimidae	<i>Dorylaimus</i> sp4	4	omnivore	0.19	0.00	0.00	0.06 (<0.01)
Dorylaimida	Tylencholaimidae	<i>Tylencholaimus</i> sp1	4	fungivore	8.48	0.91	0.60	3.33 (0.25)
Enoplida	Rhabdolaimidae	<i>Rhabdolaimus</i> sp1	3	bacterivore	36.99	9.06	23.27	23.11 (1.77)
Mononchida	Iotonchidae	<i>Iotonchus</i> sp1	4	predator	0.00	0.00	0.07	0.02 (<0.01)
Mononchida	Mononchidae	<i>Mononchus</i> sp1	4	predator	0.00	0.29	2.31	0.87 (0.07)
Mononchida	Mylonchulidae	<i>Mylonchulus</i> sp1	4	predator	0.00	0.06	0.07	0.04 (<0.01)
Monhysterida	Monhysteridae	<i>Monhystera</i> sp1	1	bacterivore	40.80	71.89	289.27	133.99 (10.25)
Plectida	Leptolaimidae	<i>Chronogaster</i> sp1	3	bacterivore	10.46	46.38	35.04	30.63 (2.34)
Rhabditida	Aphelenchoididae	<i>Aphelenchoides</i> sp2	2	fungivore	21.11	200.48	7.91	76.50 (5.85)
Rhabditida	Cephalobidae	<i>Cephalobus</i> sp1	1	bacterivore	2.58	2.18	2.46	2.41 (0.18)
Rhabditida	Panagrolaimidae	<i>Panagrolaimus</i> sp6	1	bacterivore	473.62	81.57	80.63	211.94 (16.22)
Rhabditida	Panagrolaimidae	<i>Panagrellus</i> sp1	1	bacterivore	90.50	66.01	237.94	131.48 (10.06)
Rhabditida	Pratylenchidae	<i>Hirschmanniella</i> sp1	3	herbivore	29.35	37.31	30.93	32.53 (2.49)
Rhabditida	Rhabditidae	<i>Mesorhabditis</i> sp1	1	bacterivore	1.09	0.00	0.00	0.36 (0.03)
Triplonchida	Tobrilidae	<i>Tobrilus/Epitobrilus</i> sp1	3	predator / bacterivore	159.83	79.45	51.71	97.00 (7.42)
Tylenchida	Heteroderidae	<i>Meloidogyne</i> sp1	2	herbivore	110.76	437.30	454.43	334.17 (25.57)
Tylenchida	Hoplolaimidae	<i>Helicotylenchus</i> sp1	3	herbivore	0.47	0.00	0.00	0.16 (0.01)
Tylenchida	Tylenchidae	<i>Tylenchus</i> sp1	2	herbivore	0.15	0.70	0.08	0.31 (0.02)
Identified at Family level								
Monhysterida	Monhysteridae	Monhysteridae sp2	2	bacterivore	0.33	4.67	0.55	1.85 (0.14)
Rhabditida	Aphelenchoididae	Aphelenchoididae sp3	2	herbivore	0.00	0.00	13.63	4.54 (0.35)
Rhabditida	Belonolaimidae or Merliniidae(Superfamily:Tylenchoidea)	Tylenchoidea sp1	3	herbivore	6.06	4.41	4.62	5.03 (0.38)
Rhabditida	Cephalobidae	Cephalobidae sp1	2	bacterivore	0.18	0.53	3.57	1.43 (0.11)
Rhabditida	Rhabditidae	Rhabditidae sp1	1	bacterivore	14.66	0.90	7.61	7.72 (0.59)
unidentified								
		unidentified sp1			6.82	52.07	18.75	25.88 (1.98)
		unidentified larva			0.56	8.11	21.61	10.09 (0.77)
		unidentified sp2			0.00	1.00	2.16	1.05 (0.08)
		larval Monhysteridae			0.35	10.65	1.83	4.28 (0.33)
		unidentified sp3			0.33	1.13	0.00	0.49 (0.04)
		unidentified sp4			0.36	0.42	0.00	0.26 (0.02)
Total					1217.80	1220.40	1482.16	1306.79

Molecular identification

Eleven morphospecies were collected again in 2021 (see result) for the molecular identification. For each morphospecies, 1–4 individuals were sequenced.

The nematodes, firstly killed in hot water, were morphologically identified under an inverted microscope at a magnification of 40–400x. A single nematode was isolated using pipette to a 0.2 mL PCR tube. Liquid was left to evaporate at 50°C for 10 min. The DNA extraction was performed using 10 µL QuickExtract™ DNA Extraction Solution (LGC Biosearch Technologies, Hoddesdon, UK), followed by heating at 65°C for 30 min and 98°C for 2 min. The DNA solutions were preserved at -20°C.

The partial 18s rDNA gene was amplified by PCR using the universal primers NF1

(GGTGGTGCATGGCCGTTCTTAGTT) and 18Sr2b_ExtR (GGTGTGTACAAKSGCAGGGACGTA) (Kenmotsu *et al.*, 2021). The heating cycle for PCR was 94°C for 2 min, followed by 34 cycles of 94°C for 1 min, 30°C for 30 sec, and 72°C for 1 min, with a final extension at 72°C for 1 min. PCR products were examined by electrophoresis using a 1% agarose gel before being sequenced.

The sequences were compared with the nucleotide collection (nt) in the National Center for Biotechnology Information database (NCBI, downloaded at 2021 May 17th) using Basic Local Alignment Search Tool (BLAST+ 2.14.0, Camacho *et al.*, 2009). The results were evaluated in the order of expect value (*e*-value), bit score, percentage of identical matches (*p*-ident), and alignment length.



Abundance estimation

Nematode abundance was estimated by individuals per 100 g dry soil. The number of each nematode species extracted from each soil sample was estimated from the numbers of individuals in an aliquot of 10 ml out of 13 ml nematode suspension. The moist soil, after nematode extraction, was dried for seven days at 60°C in an oven and weighted to an accuracy of 0.01 g. For the 2018 collection, nematode abundance was estimated by 400 mL wet soil samples, and the dry soil weight was estimated by the bulk density and soil moisture content provided by Aquatic Ecosystems Laboratory, National Chung Hsing University, Taichung, Taiwan.

RESULTS

Nematode taxa and their abundance

During the three-year survey, 28,051 nematodes were examined and 27,358 (97.53%, supplementary table S1) of them were characterized into 26 morphospecies from eight Orders, 17 Families, and 18 genera (Table 1).

The average abundance across the three-year survey was 13.07 individuals per 100 g dry soil. The nine most abundant morphospecies (with > 1% total estimated abundance) accounted for 92.48% of the total estimated abundance (Table 1). Bacterivore was the most abundant (49.12% of total estimated individuals) and most diverse (10 species) functional group, which is followed by herbivore (28.82%), omnivore (12.65%), fungivore/root-feeding (6.11%), and predator (0.07%). The nine most abundant morphospecies (ordered by abundance) are *Meloidogyne* sp1, *Panagrolaimus* sp6, *Dorylaimus* sp1, *Monhystera* sp1, *Panagrellus* sp1, *Tobrilus* sp1, *Aphelenchoides* sp2, *Hirschmanniella* sp1, and *Chronogaster* sp1.

Morphological description

Among the 18 nematode genera identified, nine most abundant genera (*Aphelenchoides*, *Chronogaster*, *Dorylaimus*, *Hirschmanniella*, *Meloidogyne*, *Monhystera*, *Panagrellus*, *Panagrolaimus*, *Tobrilus/Epitobrilus*) were described in more details, whereas the other nine genera (*Cephalobus*, *Helicotylenchus*, *Iotonchus*, *Mesorhabditis*, *Mononchus*, *Mylonchulus*, *Rhabdolaimus*, *Tylencholaimus*, *Tylenchus*) accounting for only 2.34% of the total estimated abundance, were roughly described according to the pictures taken at relatively lower magnification (Fig. 1–4). Five morphospecies identified only to the family level (Rhabditidae sp1, Tylenchoidea sp1, Aphelenchoididae sp3, Monhysteridae sp2, Cephalobidae sp1), which account for 1.57% the total abundance, were depicted only with pictures and without further description (Fig. 4D–M).

Order Dorylaimida

Dorylaimidae: *Dorylaimus* (Fig. 1A–I)

Body thick, 1564.89 ± 431.66 (765.92–2024.64) μm

in length and 40.94 ± 9.68 (24.55–52.54) μm in width; slightly curved ventrally; tapering gradually towards extremities but more posteriorly, usually dark in color. Lip weakly developed and flattened. Cephalic setae absent. Two odontostyle present at mouthpart and lateral esophagus, respectively; basal stylet knobs absent. Esophagus cylindrical with posterior third of esophagus swollen, basal part esophagus oval. Body cuticle thick with longitudinal ridges. Four different morphological types found. *Dorylaimus* sp1 most abundant, tail elongate to filiform (~50 μm in length) in female and rounded in male. Tails of *Dorylaimus* sp2 conoid to hemispherical and ending in a tip. Tails of *Dorylaimus* sp3 filiform and usually longer than 100 μm in length. Morphology of *Dorylaimus* sp4 closed to *Dorylaimus* sp1, but longitudinal ridges more distinct.

Tylencholaimidae: *Tylencholaimus* (Fig. 1J)

Body vermiform, straight to slightly curved, 513.15 μm in length and 22.99 μm in width. Lip slightly offset. Cephalic setae indistinct or absent. Odontostyle short, less than 100 microns. Esophagus not overlapping intestine. Basal part esophagus elongate; esophageal bulb absent. Tail rounded.

Order Enoplida

Rhabdolaimidae: *Rhabdolaimus* (Fig. 1K–M)

Body straight to slightly curved, 473.50 ± 72.40 (383.92–568.27) μm in length and 19.57 ± 3.82 (12.04–26.22) μm in width. Lip indistinct and round. Cephalic setae absent. Stoma cavity slender with sclerotized tubular walls; teeth absent. Esophagus uniformly cylindrical; valvate terminal esophageal bulb present. Vulva on mid body. Tail elongate-conoid with a tapering tail tip.

Order Mononchida

Iotonchidae: *Iotonchus* (Fig. 1N, Q)

Body thick, straight to slightly curved, 984.81 μm in length and 33.04 μm in width. Cephalic setae absent. Lip indistinct and round. Stoma cavity large, barrel-shaped. Stomal wall cuticularized with two teeth anteriorly directed in basal part of stoma. Esophagus uniformly cylindrical; pharynx muscular. Esophago-intestinal junction not overlapped. Median and terminal esophageal bulb absent. Tail tapering. Ovary paired.

Mononchidae: *Mononchus* (Fig. 1O, R, S)

Body thick, slightly curved, 961.80 μm in length and 44.48 μm in width. Anterior slightly tapering. Lip indistinct and round. Cephalic setae absent. Stoma cavity large, barrel-shaped; stomal wall cuticularized with one tooth anteriorly directed in higher third of stoma; dorsal tooth sharp, anterior with apex directed forward in cavity. Esophagus uniformly cylindrical, pharynx muscular. Esophago-intestinal junction not overlapped. Median and terminal esophageal bulb absent. Tail curved, elongate with rounded terminus.

Mylonchulidae: *Mylonchulus* (Fig. 1P, T)

Body thick, curved, 936.42 μm in length and 30.17

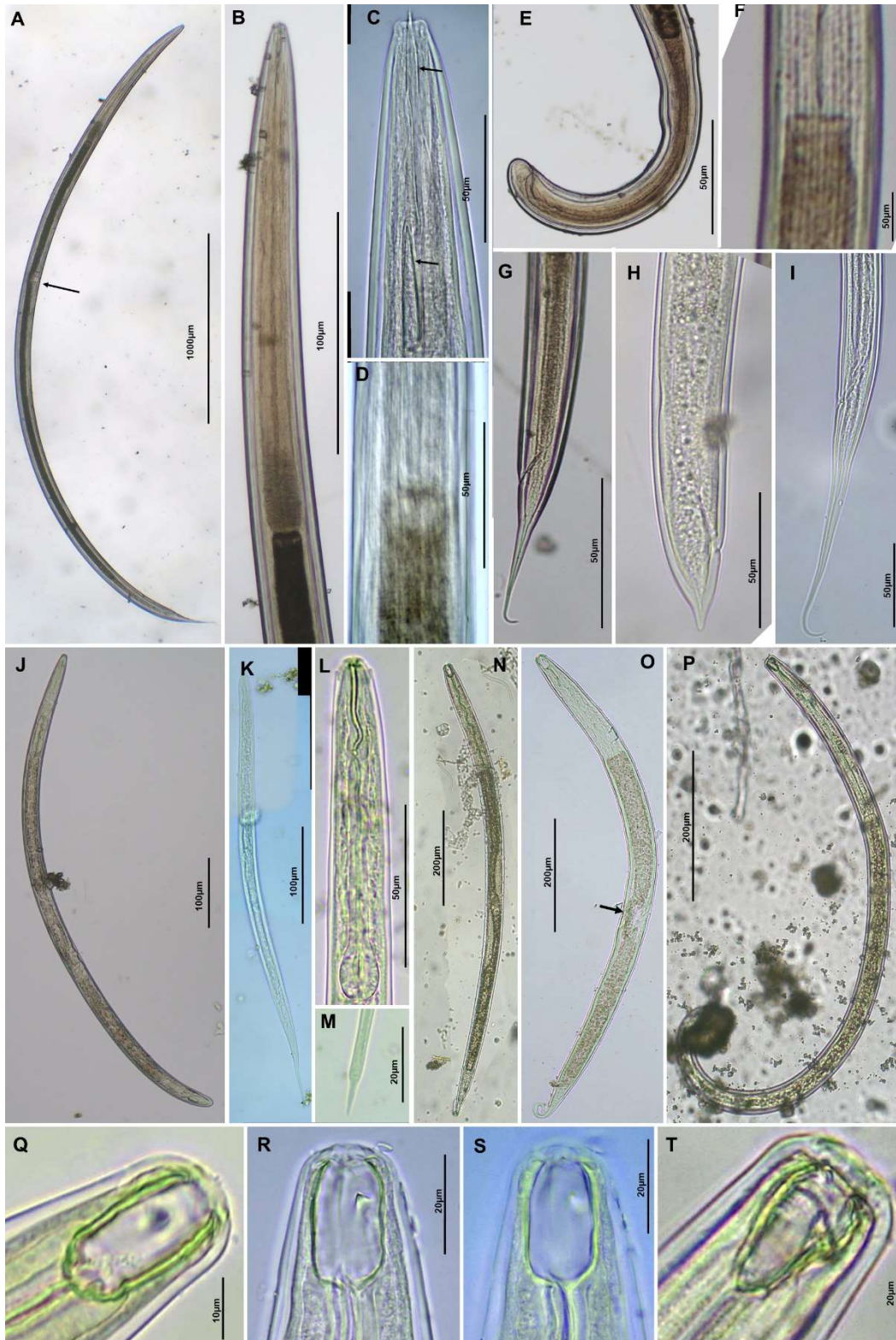


Fig 1. *Dorylaimus* (A-I), *Tylencholaimus* (J), *Rhabdolaimus* (K-M), and *Mononchida* (N-T) nematodes collected in the rice paddy field. **A.** Entire female of *Dorylaimus* sp1 with an arrow indicating the vulva; **B.** anterior region and esophagus; **C.** lip and two odontostyles (arrows); **D.** thick body cuticle with longitudinal ridges; **E.** male tail; **F.** longitudinal ridges on *Dorylaimus* sp4; **G.** female tail of *Dorylaimus* sp1; **H.** female tail of *Dorylaimus* sp2; **I.** female tail of *Dorylaimus* sp3. **J.** Entire female of *Tylencholaimus* sp1. **K.** Entire female, **L.** anterior region, and **M.** tail ending of *Rhabdolaimus* sp1. **N.** Entire female and **O.** stoma cavity of *lotonchus* sp1; **P.** entire female, **Q.** tooth in higher third of stoma wall, and **R.** dorsal tooth of *Mononchus* sp1; **S.** entire female and **T.** stoma cavity of *Mylonchulus* sp1.



μm in width. Lip indistinct and round. Cephalic setae absent. Stoma cavity large, goblet shaped; stomal wall cuticularized with one large tooth anterior directed in mid part of stoma; dorsal tooth sharp, anterior with apex directed forward in cavity. Esophagus uniformly cylindrical, pharynx muscular. Esophago-intestinal junction not overlapped. Median and terminal esophageal bulb absent. Tail elongate-conoid, ventrally curved.

Order Monhysterida

Monhysteridae: *Monhystera* (Fig. 2A–E)

Body straight to slightly curved, 615.17 ± 162.52 (422.00 – 922.40) μm in length and 26.89 ± 5.71 (19.68 – 40.30) μm in width. Lip indistinct and flattened. Cephalic setae tiny. Stoma cavity shallow and small, thin-walled and leading into funnel-shaped beginning of esophagus; teeth absent. Esophagus uniformly cylindrical with basal expansions; esophago-intestinal junction with well-developed cardia; esophageal bulb absent. Cuticle smooth with submedian setae along body. Vulva on lower third of body. Amphids distinct and circular, 1/2–1/3 head-width. Tail elongate to filiform.

Order Plectida

Leptolaimidae: *Chronogaster* (Fig. 2F–K)

Body slender, slightly open 'C'-shaped, 1110.87 ± 261.27 (716.35 – 1471.67) μm in length and 24.38 ± 5.98 (15.72 – 34.65) μm in width. Anterior gradually tapering. Lip raised and slightly offset. Cephalic setae present. Stoma cavity cylindrical; stoma wall slightly cuticular without teeth or minute; esophagus uniformly cylindrical. Anterior of basal esophageal bulb structured with jagged valves. Amphids stirrup-shaped. Female ovary monovarial. Body cuticle clearly annulated. Tail elongate-conoid.

Order Rhabditida

Aphelenchoididae: *Aphelenchoides* (Fig. 2L–P)

Body uniformly arcuate, 477.61 ± 190.39 (201.62 – 727.61) μm in length and 17.19 ± 4.82 (10.66 – 22.64) μm in width. Lip raised, offset. Cephalic setae absent. Stomatostyle slender with small, distinct knobs. Anterior part of esophagus slender and slightly distorted; Valvate median esophageal bulb circular, well-developed, nearly as large as body diameter. Vulva on lower third of body. Body cuticle smooth. Tail conoid to hemispherical and ending in a tip.

Cephalobidae: *Cephalobus* (Fig. 2Q)

Body stubby, straight, 472.86 ± 151.34 (269.71 – 683.96) μm in length and 27.27 ± 9.59 (17.00 – 43.15) μm in width. Cephalic setae absent. Lip indistinct and flattened. Stoma cavity cylindrical, narrow; stomal walls not cuticularized, teeth absent. Esophagus expanded at mid-region. valve basal esophageal bulb present. Cuticle weakly annulated. Morphology reassemble *Panagrolaimus* sp6 but different in bluntly conical tail.

Panagrolaimidae: *Panagrellus* (Fig. 2R–V)

Body eel-like, 817.02 ± 110.61 (598.21 – 1004.00) μm in length and 20.17 ± 3.41 (15.00 – 26.67) μm in width.

Lip weakly developed and flattened. Cephalic setae absent. Anterior part of stoma short cylindrical, followed with slightly open chamber; stomal wall not cuticularized; teeth absent. Esophagus expanded at mid-region, forming long tapering corpus with no offset metacarpus. Terminal esophageal bulb present. Vulva on mid body. Tail elongate to filiform with sharp terminus. Ovary monovarial and reflexed.

Panagrolaimidae: *Panagrolaimus* (Fig. 3A–G)

Body stubby, straight, 400.53 ± 155.41 (209.00 – 576.11) μm in length and 21.36 ± 7.88 (13.50 – 32.71) μm in width. Cephalic setae absent. Lip indistinct and flattened. Stoma cavity cylindrical, narrow; stomal walls not cuticularized, teeth absent. Esophagus expanded at mid-region. valve basal esophageal bulb present. Cuticle weakly annulated. Tail with sharp terminus.

Pratylenchidae: *Hirschmanniella* (Fig. 3H–M)

Body eel-like, 1944.39 ± 570.35 (1098.22 – 2677.98) μm in length and 32.75 ± 7.48 (22.45 – 42.98) μm in width. Anterior surface with moderately developed head skeleton. Cephalic setae absent. Lip raised, typically convex and amalgamated, continuous with body contour. Stomatostyle robust with rounded basal stylet knobs. Esophagus overlap and extend to the anterior end of intestine; valvate median esophageal bulb fusiform. Body cuticle smooth or slightly annulated. Vulva on mid-body. Tail elongate-conoid; tail tip mucronate. Male gubernaculum small, slightly protruding, caudal alae present.

Rhabditidae: *Mesorhabditis* (Fig. 3N–O)

Body straight to slightly curved, $760.15 \mu\text{m}$ in length and $36.67 \mu\text{m}$ in width. Lip weakly developed and flattened. Cephalic setae absent. Stoma cavity cylindrical and long without teeth. Esophagus cylindrical; valvate terminal esophageal bulb present. Cuticle slightly annulated. Tail conoid, more or less tapering.

Order Triplonchida

Tobrilidae: *Tobrilus* (Fig. 3P–U)

Body thick, 1412.41 ± 163.10 (1048.17 – 1579.95) μm in length and 47.45 ± 7.75 (31.19 – 59.83) μm in width; straight to slightly curved; tapering gradually towards extremities but more posteriorly, anterior end flattened, usually dark in color. Lip indistinct and flattened. Cephalic setae present. Stoma cavity funnel-shaped; stomal wall cuticularized, with small teeth. Esophagus uniformly cylindrical; pharynx muscular; esophageal bulb absent. Cuticle smooth with submedian setae along body. Ovary paired. Tail steadily tapering, filiform.

Order Tylenchida

Heteroderidae: *Meloidogyne* (Fig. 3V–Y)

Only free-living juveniles were collected in the soil samples due to the fact that its adult stage is a plant-root endoparasite. Body of juvenile uniformly arcuate, 458.55 ± 33.75 (393.47 – 504.22) μm in length and 15.67 ± 1.36 (13.50 – 18.25) μm in width. Lip typically convex and amalgamated, continuous with body contour. Cephalic

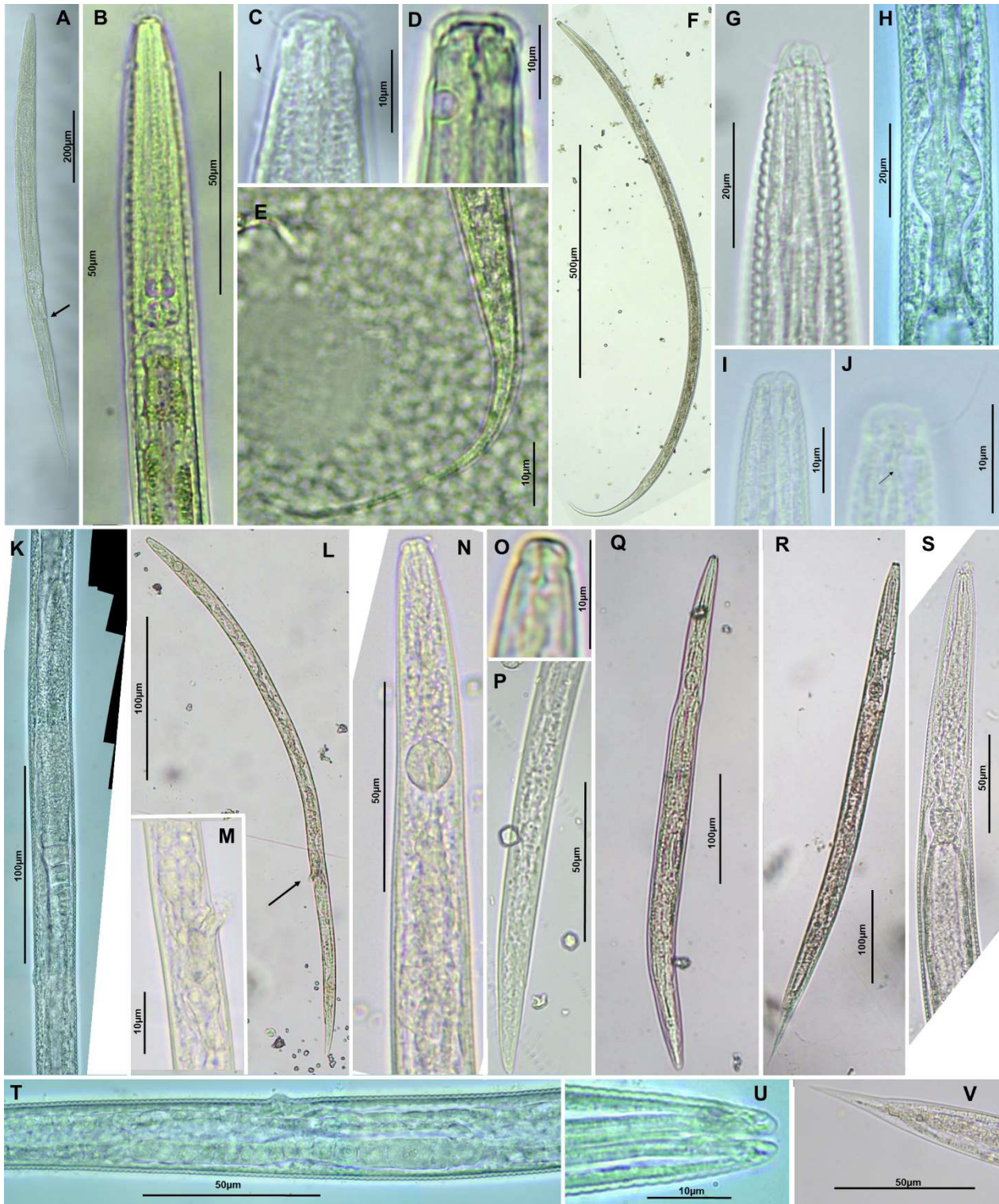


Fig. 2. *Monhystera* (A-E), *Chronogaster* (F-K), *Aphelenchoides* (L-P), *Cephalobus* (Q) and *Panagrolaimus* (R-V) nematodes collected in the rice paddy field. **A.** Entire female with an arrow indicating the vulva; **B.** anterior region and esophagus; **C.** lip cephalic setae, and submedian setae (arrow) along body; **D.** stoma cavity and circular amphid; **E.** female tail of *Monhystera* sp1. **F.** Entire female; **G.** anterior region and annulated cuticle; **H.** basal esophageal bulb; **I.** lip and stoma cavity; **J.** cephalic setae and stirrup-shaped amphids; **K.** ovary monovarial with an arrow indicating the vulva of *Chronogaster* sp1. **L.** Entire female with an arrow indicating the vulva; **M.** vulva; **N.** anterior region and median esophageal bulb; **O.** lip and stomatostyle; **P.** female tail of *Aphelenchoides* sp2. **Q.** Entire female of *Cephalobus* sp1. **R.** Entire female; **S.** anterior region and esophagus; **T.** vulva; **U.** lip and stoma cavity; **V.** female tail of *Panagrolaimus* sp6.

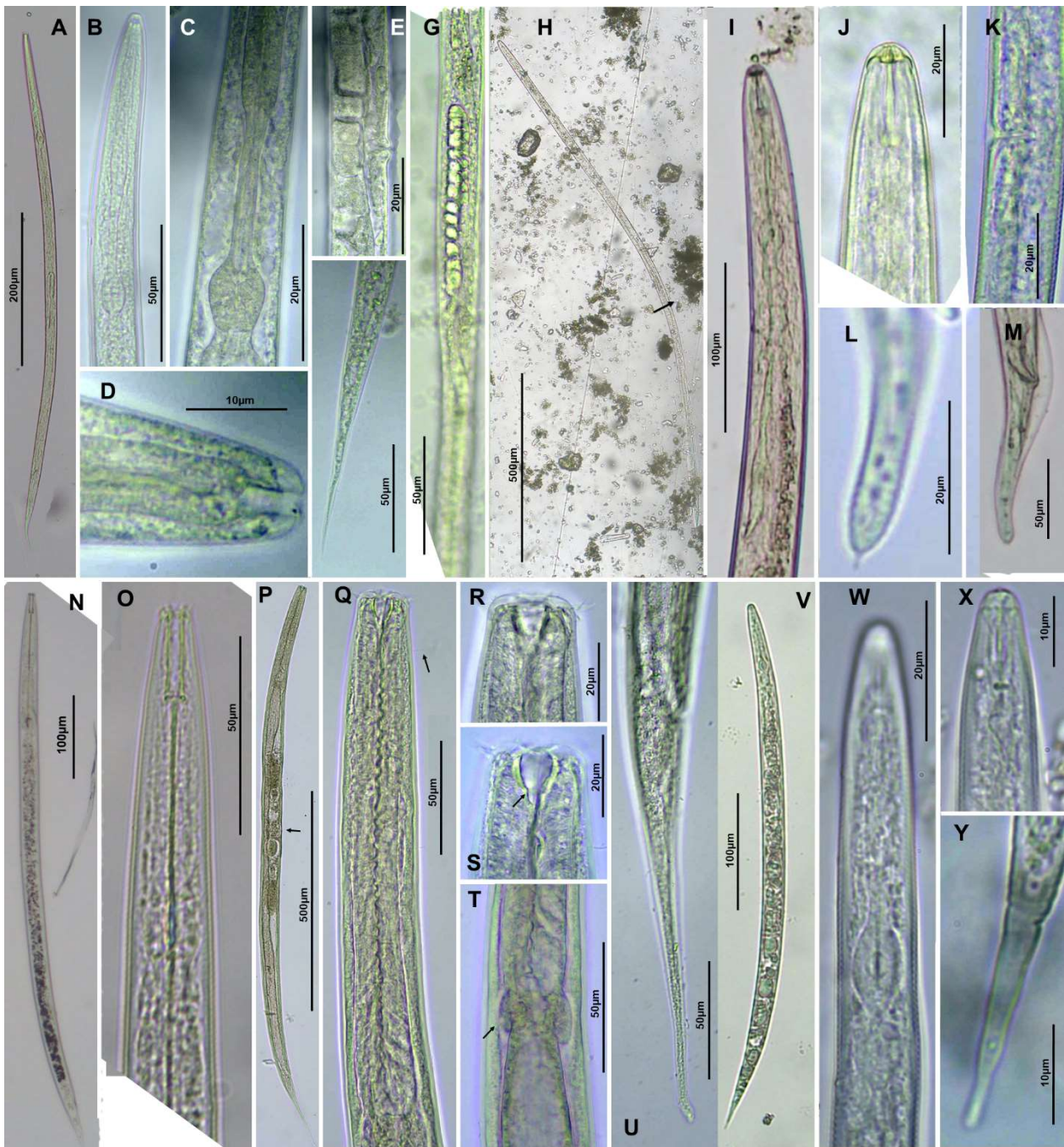


Fig. 3. *Panagrellus* (A-G), *Hirschmanniella* (H-M), *Mesorhabditis* (N-O), *Tobrilus/Epitobrilus* (P-U) and *Meloidogyne* (V-Y) nematodes collected in the rice paddy field. **A.** Entire female; **B.** anterior region and esophagus; **C.** terminal esophageal bulb; **D.** lip and stoma cavity; **E.** vulva; **F.** female tail; **G.** reflexed ovary of *Panagrellus* sp1. **H.** Entire female with an arrow indicating the vulva; **I.** anterior region and esophagus; **J.** lip and stomatostyle; **K.** vulva; **L.** female tail; **M.** male tail of *Hirschmanniella* sp1. **N.** Entire female and **O.** anterior region of *Mesorhabditis* sp1. *Tobrilus*. **P.** Entire female with an arrow indicating the vulva; **Q.** anterior region, esophagus, and submedian setae (arrow) along body; **R.** lip, cephalic setae, and stoma cavity; **S.** stoma cavity and a teeth (arrow); **T.** well-developed cardia on the esophago-intestinal junction; **U.** female tail of *Tobrilus/Epitobrilus* sp1. **V.** Entire body; **W.** anterior region and median esophageal bulb; **X.** lip and stomatostyle; **Y.** tail of a juvenile of *Meloidogyne* sp1.

**Table 2.** Molecular identification of the 11 morphospecies by partial 18s rDNA sequence

morphospecies	Accession number	Best BLAST result in NCBI	Family	Genus	expect value	bit score	% of identical matches	alignment length
<i>Aphelenchoides</i> sp2	OK330236	HQ283351.1	Aphelenchoididae	<i>Aphelenchoides</i>	2.14E-135	494	96.633	297
	OK330237	HQ283351.1	Aphelenchoididae	<i>Aphelenchoides</i>	3.43E-128	470	96.479	284
	OK330238	HQ283351.1	Aphelenchoididae	<i>Aphelenchoides</i>	9.58E-129	472	96.491	285
<i>Chronogaster</i> sp1	OK349511	KJ636360.1	Plectidae	<i>Chronogaster</i>	1.56E-141	514	99.296	284
<i>Dorylaimus</i> sp1	OK330239	KJ636402.1	Nordiidae	<i>Enchodelus</i>	5.70E-146	529	99.654	289
	OK330240	KJ636402.1	Nordiidae	<i>Enchodelus</i>	5.70E-146	529	99.654	289
<i>Hirschmanniella</i> sp1	OK330241	KP179330.1	Pratylenchidae	<i>Hirschmanniella</i>	5.70E-146	529	99.654	289
	OK330242	KF366906.1	Pratylenchidae	<i>Hirschmanniella</i>	1.25E-132	484	96.897	290
<i>Meloidogyne</i> sp1	OK330243	MN447238.1	Meloidogynidae	<i>Meloidogyne</i>	5.32E-136	496	100	268
<i>Monhystera</i> sp1	OK330244	FJ969130.1	Monhysteridae	<i>Monhystera</i>	2.10E-150	544	99.663	297
<i>Panagrellus</i> sp1	OK330245	KJ434175.1	Panagrolaimidae	<i>Propanagrolaimus</i>	2.14E-61	248	87.736	212
	OK330246	AY295810.1	Protostrongylidae	<i>Muellerius</i>	5.65E-12	84.2	74.429	219
	OK330247	KJ434175.1	Panagrolaimidae	<i>Propanagrolaimus</i>	2.38E-60	244	88.889	198
<i>Panagrolaimus</i> sp6	OK330248	GU014546.1	Panagrolaimidae	<i>Panagrolaimus</i>	4.63E-122	449	98.431	255
<i>Tobrilus/Epitobrilus</i> sp1	OK330250	KJ636217.1	Tobrilidae	<i>Epitobrilus</i>	2.71E-144	523	98.649	296
	OK330251	KJ636217.1	Tobrilidae	<i>Epitobrilus</i>	3.38E-138	503	98.596	285
	OK330252	KJ636217.1	Tobrilidae	<i>Epitobrilus</i>	3.38E-138	503	98.596	285
	OK330253	KJ636217.1	Tobrilidae	<i>Epitobrilus</i>	2.64E-139	507	98.606	287
<i>Cephalobus</i> sp1 ¹	OK330254	AF202161.1	Cephalobidae	<i>Cephalobus</i>	1.46E-153	555	99.346	306
<i>Rhabdolaimus</i> sp1 ²	OK330249	KY822951.1	-	-	3.36E-34	158	80.645	217

¹ *Cephalobus* sp1 is originally identified as the same genus with *Panagrolaimus* sp6 but isolated according to the tail shape. The molecular data suggests a reliable result with the high sequence similarity and thus provided with the other predominant species.

² *Rhabdolaimus* sp1 is the tenth most abundant morphospecies.

setae absent. Stomatostyle slender with small, distinct knobs. Anterior part of esophagus slender and slightly distorted; valvate median esophageal bulb fusiform. Body cuticle slightly annulated. Tail conoid, more or less tapering, but not elongate-filiform.

Hoplolaimidae: *Helicotylenchus* (Fig. 4A)

Body vermiform, spiral, 623.24 µm in length and 24.33 µm in width. Cephalic setae indistinct or absent. Lip raised, typically convex and amalgamated, continuous with body contour. Stomatostyle short with basal stylet knobs. Valvate median esophageal bulb present. Tail round with a terminal ventral process.

Tylenchidae: *Tylenchus* (Fig. 4B–C)

Body straight to slightly curved, 835.64 µm in length and 27.53 µm in width; tapering gradually towards anterior end. Cephalic setae indistinct or absent. Lip raised, slightly offset. Stomatostyle short with basal stylet knobs. Esophagus not overlapping intestine. Valvate median esophageal bulb present. Median esophageal bulb distinct but not well-developed. Tail filiform.

Molecular identification

In 2021, eleven morphospecies were collected for molecular identification to complement morphological data. The results showed that morphological identifications aligned with molecular identifications to the family level for nine species and to the genus level for seven species (*Aphelenchoides* sp2, *Cephalobus* sp1, *Chronogaster* sp1, *Hirschmanniella* sp1, *Meloidogyne* sp1, *Monhystera* sp1, and *Panagrolaimus* sp6). The sequence identity (p-ident) for these seven morphospecies ranged from 96.479% to

100% (Table 2).

Four morphospecies (*Dorylaimus* sp1, *Panagrellus* sp1, *Rhabdolaimus* sp1, *Tobrilus* sp1) showed inconsistency between morphological and molecular identifications, possibly due to the highly conserved sequences in the 18S rDNA gene. Additionally, the accuracy of BLAST results heavily relies on whether closely related taxa have undergone sequence examinations. The BLAST results for *Dorylaimus* sp1 sequences revealed a 99.654% sequence identity with *Enchodelus* spp. (Dorylaimida: Nordiidae). Despite the high similarity, we maintained our classification based on a significant morphological difference: the tail shape is round in *Enchodelus* but filiform in our specimens. In addition, the two *Dorylaimus* sp1 sequences also showed high similarity (p-ident >98%) to the sequences identified as other families (Actinolaimidae, Aporcelaimidae, Dorylaimidae, Qudsianematidae), including those of *Paractinolaimus* (e.g. accession number: AY552975.1), *Amblydorylaimus* (KM092519.1), *Mesodorylaimus* (AY146514.2), *Aporcelinus* (MN727056.1), *Dorylaimus* (AY284777.1), and *Ecumenicus* (MK292127.1). The observed inconsistencies, even at the family level, suggest a potential taxonomic complexity within this group or a limitation in the resolution of the 18S rDNA gene for identifying these taxa. Therefore, we will adhere to our morphological classification until new data suggest otherwise.

For *Tobrilus* sp1, the BLAST results are identified as the close related genus, *Epitobrilus*. However, a sequence from *Tobrilus* sp. (JQ429745.1) displayed an even higher

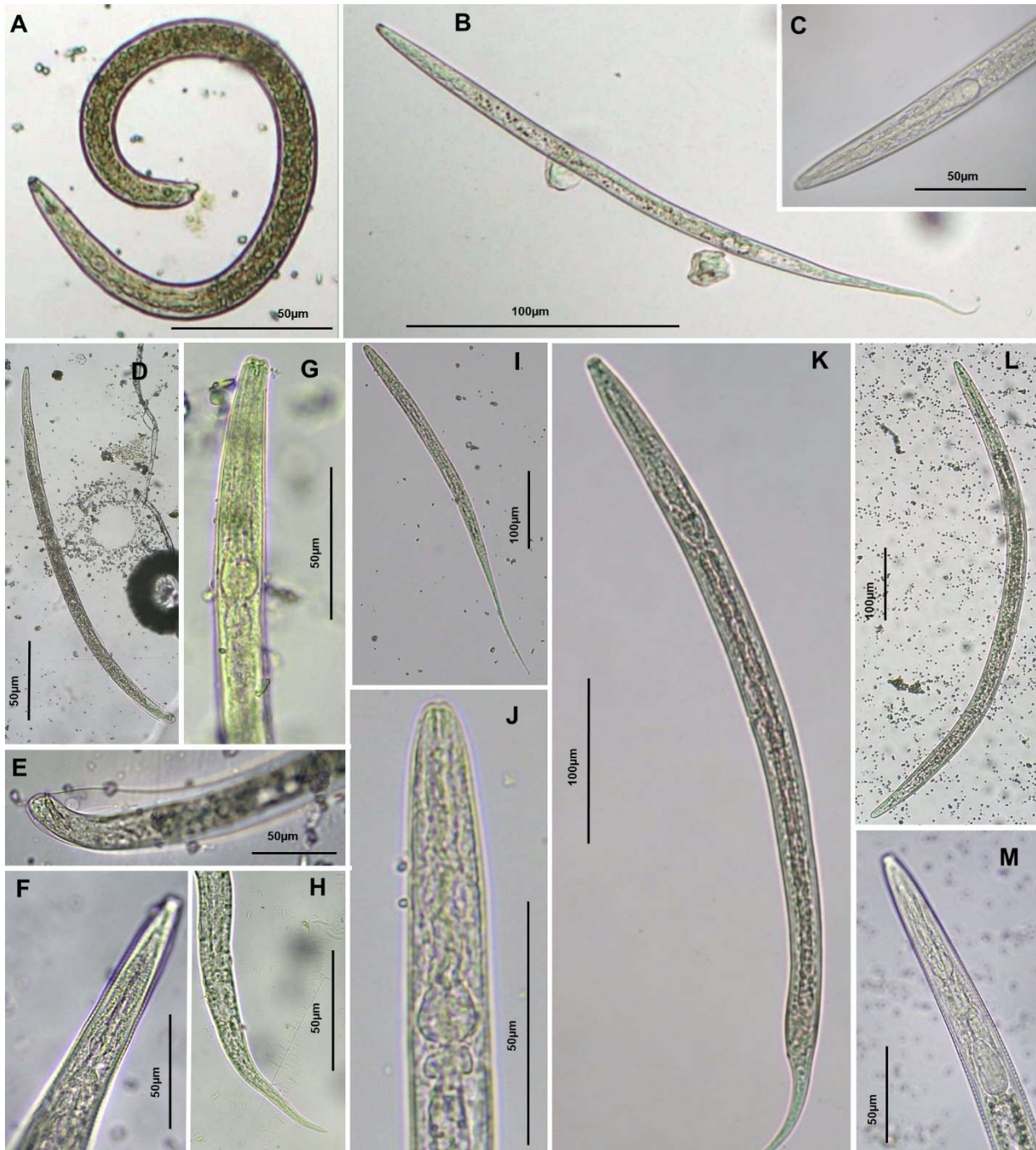


Fig 4. *Helicotylenchus* (A), *Tylenchus* (B-C), *Aphelenchoididae* (D-F), *Cephalobidae* (G-H), *Monhysteridae* (I-J), *Rhabditidae* (K), and *Tylenchoidea* (L-M) nematodes collected in the rice paddy field. A. entire female of *Helicotylenchus* sp1. B. entire female and C. anterior region of *Tylenchus* sp1. D. Entire male, E. anterior region, and F. tail of *Aphelenchoididae*. G. Anterior region and H. female tail of *Cephalobidae*. I. Entire body, and J. anterior region *Monhysteridae*. K. Entire body of *Rhabditidae*. L. Entire body, and M. anterior region of *Tylenchoidea*.

similar (98.93%) but also with the higher e-value (ranged from $7e-131$ to $6e-125$) to our samples. The morphology is similar in these two genera while *Epitobrilus* was structured with obvious supplements on the posterior part of the male (Naumova and Gagarin, 2017). Because such structure was not clearly reported in our samples, the

genus of *Tobrilus* sp1 is currently judged as *Tobrilus/Epitobrilus*.

The BLAST results for *Panagrellus* sp1 and *Rhabdolaimus* sp1 failed to provide reliable taxonomic evidence, as no hits with more than 90% identity were found. Currently, *Panagrellus* sp1 (family Panagrolaimidae) is



classified based on all four morphological keys used in this study, however, it cannot be corroborated by molecular analysis due to the lack of available public sequence data. Therefore, we have adhered to the morphological classification and proposed the taxonomic status of *Panagrellus* sp1 and *Rhabdolaimus* sp1, pending verification from forthcoming data.

DISCUSSION

Species components in the rice paddy field

Nematode communities have long been utilized as bioindicators, effectively reflecting the food web structure and soil conditions (Yeates *et al.*, 1993; Bongers and Bongers, 1998; Ferris, 2010). A well described nematode fauna can facilitate the use of nematode communities as bioindicators. In this study, 18 genera were identified from the rice paddy fields. While eleven of these genera were previously recorded in the survey of soil nematodes in Taiwan (Ho, 2011; Jhao, 2013), seven of them (*Dorylaimus*, *Meloidogyne*, *Monhystera*, *Mononchus*, *Rhabdolaimus*, *Tobrilus/Epitobrilus*, *Tylenchus*) are newly recorded here. Although the nematodes are found in the rice paddy fields, they can be recruited from the surrounding area. As most of the agricultural ecosystems which are highly linked to the surrounding ones (Bambaradeniya and Amerasinghe, 2003), these nematodes also inhabit surrounding environments, enabling them to cycle between flooded and terrestrial habitats. We hypothesize that the succession of nematodes in rice paddies could result from the influx of nematode populations from surrounding environments into the paddies, leading to population dynamics changes with the rice cultivation process.

Comparisons between nematode fauna from rice paddy fields in seven regions across China, Japan, Russia, and Vietnam (Ishibashi *et al.*, 1983; Liu *et al.*, 2008; Okada *et al.*, 2011; Liu *et al.*, 2016ab; Okada *et al.*, 2016; Korobushkin *et al.*, 2019; Van Nguyen *et al.*, 2020; Yang *et al.*, 2020) showed that 15 genera are commonly found (in at least five of the seven regions). Of these, 11 of them (*Aphelenchoides*, *Cephalobus*, *Chronogaster*, *Dorylaimus*, *Helicotylenchus*, *Hirschmanniella*, *Mesorhabditis*, *Mononchus*, *Panagrolaimus*, *Tobrilus/Epitobrilus*, *Tylenchus*) were also identified in this study. Notably, the two herbivorous genera, *Aphelenchoides* and *Hirschmanniella*, were present in all seven studies, and *Aphelenchoides* was also detected in the survey of plant-feeding nematodes in Kenya (Namu *et al.*, 2018). In contrast, *Iotonchus* and *Panagrellus* are documented in the rice paddy fields for the first time. Among the 18 genera we identified, the nematode community composition in Taiwan closely resembles those in Vietnam (Van Nguyen *et al.*, 2020) and Jiangsu, China (Liu *et al.*, 2016ab), where 14 of the genera were also detected. This contrasts with the fewer overlapping

genera (5-9 genera) observed in the other regions (Ishibashi *et al.*, 1983; Liu *et al.*, 2008; Okada *et al.*, 2011; Okada *et al.*, 2016; Korobushkin *et al.*, 2019; Yang *et al.*, 2020).

Functional group of the predominated species

Among the 26 identified morphospecies, over 94% of the population comprises the ten most abundant species, which could be indicative of the main ecological function in the field. Of these, six are characterized as bacterivores (*Chronogaster*, *Monhystera*, *Panagrellus*, *Panagrolaimus*, *Rhabdolaimus*, and *Tobrilus/Epitobrilus*), representing the most diverse functional group, which can be further categorized into *cp1* (*Monhystera*, *Panagrolaimus*, *Panagrellus*, *Rhabdolaimus*) and *cp3* (*Chronogaster*, *Tobrilus/Epitobrilus*) nematodes. *Cp1* nematodes were reported with short generation time and high fecundity, which could therefore be a plausible explanation for their higher abundance. Temporal dynamics of the bacterivores are highly correlated with the bacterial abundance and application of fertilizer (Ferris, 2010), which can explain predominance of the *cp1* nematodes in the highly disrupted environment culturing rice. The feeding habit of the *cp3* bacterivore, *Tobrilus/Epitobrilus*, is considered as both predator (Yeates *et al.*, 1993) and bacterivore (e.g. Okada *et al.*, 2011). Some predacious nematodes switch to feed on bacteria in the absence of prey nematodes (Khan and Kim, 2007). This might explain why the cuticularized stroma wall with small tooth in *Tobrilus/Epitobrilus* resembles that of predators, whereas the cephalic setae are similar to those of bacterivores. Rice paddy fields are a flooded environment and are highly selective to the nematodes that are more adaptive to aquatic environment. The influence of flooding on different nematode species has been noted in Okada *et al.* (2016). Three nematode genera found in this study were also recorded in Okada *et al.* (2016): *Rhabdolaimus* and *Tobrilus* were found more frequently in the aquatic environment, while *Chronogaster* were found in both terrestrial and rice paddy (aquatic) fields.

Aphelenchoides is the most commonly found nematodes globally in the rice paddy field (Ishibashi *et al.*, 1983; Liu *et al.*, 2008; Okada *et al.*, 2011; Liu *et al.*, 2016ab; Okada *et al.*, 2016; Korobushkin *et al.*, 2019; Van Nguyen *et al.*, 2020; Yang *et al.*, 2020). Although *Aphelenchoides* typically functions as a fungivore under normal circumstances, it can adapt to various conditions and exhibit plant root feeding behavior (Hooper and Cowland, 1986; Yeates *et al.*, 1993). Additionally, certain species within the genus, such as *A. varicaudatus* (Maharani *et al.*, 2023), are known to attack plant roots, while others, like *A. besseyi* (Karssen and Groza, 2018), are notorious for their pathogenic impact on the upper parts of rice plants. *Aphelenchoides* and *Tylencholaimus*, the only two fungivores found in this study, are in low abundance, which might suggest that bacteria in rice



paddy field plays a more crucial role in transferring energy to high level of the food web.

Two herbivores (plant pathogenic nematodes), *Meloidogyne* and *Hirschmanniella*, were found in this study, while the former one being the most abundant nematode among all genera. Although adult *Meloidogyne* behaves as a sedentary endoparasite within plant roots, its juveniles are free-living (infective) and actively seek out new hosts in the soil. The DNA sequence of *Meloidogyne* collected in this study is identical to that of *M. graminicola*. Despite pathogenic nematodes for rice likely to be similar around the world, particularly in the Asia (Mantelin *et al.*, 2017), rice fields were not sampled in most of the previous surveys except Vietnam (Van Nguyen *et al.*, 2020) and Kenya (Namu *et al.*, 2018). Among these studies, *Hirschmanniella* is more frequently detected in the rice paddy fields (Ishibashi *et al.*, 1983; Liu *et al.*, 2008; Okada *et al.*, 2011; Liu *et al.*, 2016ab; Okada *et al.*, 2016; Korobushkin *et al.*, 2019; Van Nguyen *et al.*, 2020; Yang *et al.* 2020). *Hirschmanniella* is a root endoparasite attacking plant roots. Population dynamics of *Hirschmanniella* are highly correlated with the rice growth, which reaches the highest peak during the soft dough stage (booting, heading, flowering, milking) and starts to decrease in (hard) dough stage (Islam *et al.*, 2004; Maung *et al.*, 2013; Win *et al.*, 2013). Across the three-year survey, the estimated abundance of *Hirschmanniella* is more consistent comparing to nine other predominant nematodes. It might suggest that the population dynamics of *Hirschmanniella* are more consistent through the years or the spatial pattern is more homogeneous in the field.

Dorylaimus is a large indiscriminate omnivore (Zheng *et al.*, 2019) which can even facultatively prey on other nematodes encountered by the hollow-spear (Linford and Oliveira, 1937; Shafqat *et al.*, 1987). It is a dominant soil nematode in flooded field (Okada *et al.*, 2011; Zheng *et al.*, 2019) and also the most found omnivore in the global survey of rice paddy fields (Ishibashi *et al.*, 1983; Liu *et al.*, 2008; Okada *et al.*, 2011; Liu *et al.*, 2016ab; Okada *et al.*, 2016; Korobushkin *et al.*, 2019; Van Nguyen *et al.*, 2020; Yang *et al.* 2020). As a common nematode in the agriculture system, *Dorylaimus* is frequently studied, including the research on the effect of fertilization on symbiotic bacteria in *Dorylaimus* (Zheng *et al.*, 2019), or that it showed less response to plant secondary metabolites compared to phytoparasitic nematode (Chen *et al.*, 2017). However, the impact of the tillage on *Dorylaimus* population is still under-researched.

Morphological and molecular identification

Molecular techniques have long been pivotal in the nematode identification, which play a crucial role in uncovering cryptic species (e.g. Blouin, 2002) and facilitating phylogenetic studies (Ahmed *et al.*, 2015). Recent advances include the widespread adoption of

metabarcoding in the characterization of nematode communities (e.g. Treonis *et al.*, 2018). Currently, the 18s rDNA gene is the most widely used marker, covering most nematode species in the NCBI database. While it is conserved (i.e., with low genetic variation) and yields low species-level resolution, it still provides valuable information for distinguishing nematode genera and families (Ahmed *et al.*, 2019), aligning well with bioindicator frameworks that rely on identification only to the genus or family level. (Ferris *et al.*, 2001; Chen *et al.*, 2014). Several primer sets have been extensively tested for their universal adaptability in amplifying the 18s rDNA gene segment across diverse nematode species (e.g. Ahmed *et al.*, 2019; Waeyenberge *et al.*, 2019; Sikder *et al.*, 2020; Kawanobe *et al.*, 2021; Kenmotsu *et al.*, 2021). For instance, the success in amplifying 18s rDNA across well-known nematode species has been well documented (Porazinska *et al.*, 2009; Waeyenberge *et al.*, 2019). However, species composition estimated according to morphology, 18s rDNA genes barcoding, and metabarcoding displayed a very low overlap in Schenk *et al.* (2019). Kenmotsu *et al.* (2021) compared four primer sets for amplifying the 18s rDNA gene and found that two of them (SSU18A-4F3 + SSU_R22 and NF1 + 18Sr2b_ExtR) were able to amplify a relatively broader range of nematode taxa, with the latter one suggested as more efficient in Sikder *et al.* (2020). Therefore, we adopted the same primer set (NF1 + 18Sr2b_ExtR) that performed well for the for our molecular analysis. Sequences from nine of the 11 nematodes had hits with high sequence identities (> 96%) in the BLAST results, further confirming their morphological identification. However, sequences with low identities (< 90%) were found for two nematodes, and one sequence was inconsistent with morphological analyses, suggesting a lack of information for closely related nematodes in GenBank. The identification of these three nematode morphospecies requires further consideration. In addition, 27 out of 47 sequences amplified from our nematode samples are likely to be contaminated by other organisms, including annelid, fungi, and eukaryotes (data not shown). Amplification of non-target DNA has also been documented in Waeyenberge *et al.* (2019).

Characterizing nematode communities using molecular techniques offers a lower cost in labor and training compared to time-consuming morphological-based analyses. Sequence comparison also reliably predicts the closely related taxa of novel nematode species. However, recent studies have shown significant inconsistency between results obtained from molecular techniques and traditional morphological methods (Pantó *et al.*, 2021; Schenk *et al.*, 2019; Treonis *et al.*, 2018). These discrepancies in identification can significantly impact the measurements of biodiversity and functional groups, ultimately leading to divergent interpretations of



the ecological significance attributed to the nematode community (Pantó *et al.*, 2021).

CONCLUSION

Free-living nematodes have long served as indicators for monitoring soil ecosystems. Various bioindicators have been developed, taking nematode feeding behaviors and life history traits into account (Bongers and Bongers, 1998). In the present study, we have characterized the nematode community in the rice paddy fields. We identified a total of 27 morphospecies, with 11 of them further provided with molecular barcodes of 18 rDNA. Notably, nine of the morphospecies accounted for more than 94% of the nematode population, with bacterivores being predominant. Therefore, rather than aggregating data from all species to calculate bioindicators, focusing on the dynamics of the predominant nematodes may more accurately reflect the food web structure within the rice paddy field. In this study, we detailed the morphology of these dominant nematodes. As an initial step, it is valuable to extend our research to examine the species components in similar environments across Taiwan and explore their utility in monitoring soil conditions affected by various farming practices.

AUTHOR CONTRIBUTIONS

MCC, ZHL, HWC designed the study. MCC, ZHL, TWL carried out the sample collection and experiments. MCC, TWL conducted the statistical analysis and data visitation. MCC, LYL, PWH conducted the molecular examination and analysis. MCC, TWL, HWC wrote the final version of the manuscript. All authors read and approved the final version of the manuscript.

ACKNOWLEDGMENTS

This work was supported by grants from the Ministry of Science and Technology, Taiwan (MOST 109-2811-B-018-500, MOST 110-2811-B-018-001, and NSTC 112-2313-B-002-056 to Ming-Chung Chiu and MOST 106-2621-M-415 -001, 107-2621-M-415-001 to Hsuan-Wien Chen)

LITERATURE CITED

- Ahmed, M., Sapp, M., Prior, T., Karssen, G., Back, M. 2015 Nematode taxonomy: from morphology to metabarcoding. *Soil Discuss.* **2**: 1175–1220.
- Ahmed, M., Back, M.A., Prior, T., Karssen, G., Lawson, R., Adams, I., Sapp, M. 2019 Metabarcoding of soil nematodes: the importance of taxonomic coverage and availability of reference sequences in choosing suitable marker(s). *MBMG* **3**: e36408.
- Andriuzzi, W.S., Wall, D.H. 2018 Grazing and resource availability control soil nematode body size and abundance-mass relationship in semiarid grassland. *J. Anim. Ecol.* **87**(5): 1407–1417.
- Bambaradeniya, C.N.B., Amerasinghe, F.P. 2003 Biodiversity associated with the rice field agroecosystem in Asian countries: a brief review. Colombo, Sri Lanka: International Water Management Institute (IWMI). iii, 24p. (IWMI Working Paper 063)
- Barker, K., Carter, C., Sasser, J. 1985 Nematode extraction and bioassays. *In*: Barker, K.R., Carter, C.C., Sasser, J.N. (eds.). An advanced treatise on *Meloidogyne*, vol. II Methodology. 19–35. State University Graphics, Raleigh, NC, North Carolina.
- Blouin, M.S. 2002 Molecular prospecting for cryptic species of nematodes: mitochondrial DNA versus internal transcribed spacer. *Int. J. Parasitol.* **32**(5): 527–531.
- Bongers, T. 1990 The maturity index: an ecological measure of environmental disturbance based on nematode species composition. *Oecologia* **83**(1): 14–19.
- Bongers, T., Bongers, M. 1998 Functional diversity of nematodes. *Appl. Soil Ecol.* **10**(3): 239–251.
- Camacho, C., Coulouris, G., Avagyan, V., Ma, N., Papadopoulos, J., Bealer, K., Madden, T.L. 2009 BLAST+: architecture and applications. *BMC Bioinform.* **10**: 421.
- Chen, C. L., Chen, B. H., Huang, S. N., King, H. B., Sun, W. C., Guo, H. Y., Chien, C. C., Lin, R. H., Young, C. C., Chen, Z. S. 2009. Establishment and Perspectives of a Long Term Ecological Research in Agricultural Ecosystem in Subtropics. *Crop, Environment & Bioinformatics* **6**(4): 233–246.
- Chen, J., Ferris, H. 1999 The effects of nematode grazing on nitrogen mineralization during fungal decomposition of organic matter. *Soil Biol. Biochem.* **31**(9): 1265–1279.
- Chen, Q., Yang, B., Liu, X., Chen, F., Ge, F. 2017 Long-term cultivation of Bt rice expressing the Cry1Ab/1Ac gene reduced phytoparasitic nematode abundance but did not affect other nematode parameters in paddy fields. *Sci. Total Environ.* **607-608**: 463–474.
- Chen, Y.F., Han, X.M., Li, Y. F., Hu, C. 2014 Approach of nematode fauna analysis indicate the structure and function of soil food web. *Acta Ecol. Sin.* **34**(5): 1072–1084. [in Chinese with English abstract]
- De Ley, P. 2000 Lost in worm space: phylogeny and morphology as road maps to nematode diversity. *Nematology* **2**(1): 9–16.
- de Miranda, M., Fonseca, M., Lima, A., de Moraes, T., Aparecido Rodrigues, F. 2015 Environmental impacts of rice cultivation. *Am. J. Plant Sci.* **6**(12): 2009–2018.
- Edirisinghe, J.P., Bambaradeniy, C. 2006 Rice fields: an ecosystem rich in biodiversity. *JNSF.* **34**(2): 57–59.
- Ferris, H., Venette, R.C., van der Meulen H.R., Lau, S.S. 1998 Nitrogen mineralization by bacterial-feeding nematodes: verification and measurement. *Plant Soil* **203**(2): 159–171.
- Ferris, H. 2010 Form and function: Metabolic footprints of nematodes in the soil food web. *Eur. J. Soil Biol.* **46**(2): 97–104.
- Ferris, H., Bongers, T., de Goede, R.G. M. 2001 A framework for soil food web diagnostics: extension of the nematode faunal analysis concept. *Appl. Soil Ecol.* **18**(1): 13–29.
- Gebremikael, M.T., Steel, H., Buchan, D., Bert, W., de Neve, S. 2016 Nematodes enhance plant growth and nutrient uptake under C and N-rich conditions. *Sci. Rep.* **6**(1): 32862.



- George, P.B.L., Lindo, Z.** 2015 Application of body size spectra to nematode trait-index analyses. *Soil Biol. Biochem.* **84**: 15–20.
- Grove, D.I.** 1990 A history of human helminthology. CAB International, Wallingford, UK. 848pp.
- Ho, T.Y.A.** 2011 Soil nematode abundance and diversity along an altitudinal gradient in Central Taiwan. [Unpublished master's thesis] Department of Life Sciences, National Cheng Kung University, Tainan, Taiwan. 34pp.
- Hooper, D.J., Cowland, J.A.** 1986 Fungal hosts for the chrysanthemum nematode, *Aphelenchoides ritzemabosi*. *Plant Pathol.* **35**(1): 128–129.
- Ishibashi, N., Kondo, E., Ito, S.** 1983 Effects of application of certain herbicides on soil nematodes and aquatic invertebrates in rice paddy fields in Japan. *Crop Prot.* **2**(3): 289–304.
- Islam, M.S., Ahmad, M.U., Haque, A.H.M.M., Sarker, M.E.H.** 2004 Population dynamics of *Hirschmanniella oryzae* in the rice root of farmer fields as affected by edaphic factors. *PJBS.* **7**(11): 2002–2004.
- Jatala, P.** 1986 Biological control of plant-parasitic nematodes. *Annu. Rev. Phytopathol.* **24**(1): 453–489.
- Jhao, J.S.** 2013 The effects of tillage and rotation on soil nematode community in different depth. [Unpublished master's thesis] Department of Life Sciences, National Cheng Kung University, Tainan, Taiwan. 60pp.
- Kanwar, R.S., Patil, J.A., Yadav, S.** 2021 Prospects of using predatory nematodes in biological control for plant parasitic nematodes—A review. *Biol. Control.* **160**: 104668.
- Karssen, G., Groza, M.** 2018 First report of the plant-parasitic nematode *Aphelenchoides besseyi* (Nematoda: Aphelenchoididae) on rice in Romania. *Bulletin OEPP/EPPO Bulletin* **48**(2): 254–255.
- Kawanobe, M., Toyota, K., Ritz, K.** 2021 Development and application of a DNA metabarcoding method for comprehensive analysis of soil nematode communities. *Appl. Soil Ecol.* **166**: 103974.
- Kaya, H.K., Gaugler, R.** 1993 Entomopathogenic nematodes. *Annu. Rev. Entomol.* **38**(1): 181–206.
- Kenmotsu, H., Ishikawa, M., Nitta, T., Hirose, Y., Eki, T.** 2021 Distinct community structures of soil nematodes from three ecologically different sites revealed by high-throughput amplicon sequencing of four 18S ribosomal RNA gene regions. *PLoS ONE* **16**(4): e0249571.
- Khan, Z., Kim, Y.H.** 2007 A review on the role of predatory soil nematodes in the biological control of plant parasitic nematodes. *Appl. Soil Ecol.* **35**(2): 370–379.
- Korobushkin, D.I., Butenko, K.O., Gongalsky, K.B., Saifutdinov, R.A., Zaitsev, A. S.** 2019 Soil nematode communities in temperate rice-growing systems. *European J. Soil Biol.* **93**: 103099.
- Liao, C.Y.** 2012 Dynamics of Soil Nematode Communities under Conventional and Organic Tea Gardens in Central Taiwan. [Unpublished master's thesis] Department of Life Sciences, National Cheng Kung University, Tainan, Taiwan. 38pp.
- Linford, M.B., Oliveira, J.M.** 1937 The feeding of hollow-spear nematodes on other nematodes. *Science* **85**(2203): 295–297.
- Liu, M., Chen, X., Qin, J., Wang, D., Griffiths, B., Hu, F.** 2008 A sequential extraction procedure reveals that water management affects soil nematode communities in paddy fields. *Appl. Soil Ecol.* **40**(2): 250–259.
- Liu, T., Whalen, J.K., Shen, Q., Li, H.** 2016a Increase in soil nematode abundance due to fertilization was consistent across moisture regimes in a paddy riceupland wheat system. *Eur. J. Soil Biol.* **72**: 21–26.
- Liu, T., Li, Y., Shen, Q., Li, H.X., Whalen, J.** 2016b Soil nematode community response to fertilisation in the root-associated and bulk soils of a rice-wheat agroecosystem. *Nematology* **18**(6): 727–741.
- Maharani, R., Indarti, S., Soffan, A., Hartono, S.** 2023 *Aphelenchoides varicaudatus* (Nematoda: Aphelenchoididae) and *Helicotylenchus erythrinae* (Nematoda: Hoplolaimidae) from garlic plantation in Magelang, Central Java, Indonesia. *Helminthologia* **60**(1): 94–105.
- Mantelin, S., Bellafiore, S., Kyndt, T.** 2017 *Meloidogyne graminicola*: a major threat to rice agriculture. *Mol. Plant Pathol.* **18**(1): 3–15.
- Maung, Z.T.Z., Win, P.P., Kyi, P.P., Myint, Y.Y., De Waele, D.** 2013 Population dynamics of the rice root nematode *Hirschmanniella oryzae* on monsoon rice in Myanmar. *Arch. Phytopathol. Pflanzenschutz* **46**(3): 348–356.
- Min, S., Rulik, M.** 2020 Effects of different water management and fertilizer applications on CO₂ fluxes from a selected Myanmar Rice (*Oryza sativa* L.) cultivar. *Int. J. Plant Sci.* **32**(19): 22–37.
- Namu, J., Karuri, H., Alakonya, A., Nyaga, J., Njeri, E.** 2018 Distribution of parasitic nematodes in Kenyan rice fields and their relation to edaphic factors, rainfall and temperature. *Trop. Plant Pathol.* **43**(2): 128–137.
- Naumova, T.V., Gagarin, V.G.** 2017 *Tobrilus saprophagus* sp. n. and *Epitobrilus interstitialis* sp. n. (Nematoda, Triplonchida) from Lake Baikal, Russia. *Zootaxa* **4353**: 133–145.
- Neher, D.A.** 2001 Role of nematodes in soil health and their use as indicators. *J. Nematol.* **33**: 161–168.
- Okada, H., Niwa, S., Takemoto, S., Komatsuzaki, M., Hiroki, M.** 2011 How different or similar are nematode communities between a paddy and an upland rice fields across a flooding–drainage cycle? *Soil Biol. Biochem.* **43**: 2142–2151.
- Okada, H., Niwa, S., Hiroki, M.** 2016 Nematode fauna of paddy field flooded all year round. *Nematological Research* **46**: 65–70.
- Pantó, G., Pasotti, F., Macheriotou, L., Vanreusel, A.** 2021 Combining traditional taxonomy and metabarcoding: Assemblage structure of nematodes in the shelf sediments of the eastern Antarctic Peninsula. *Front. mar. sci.* **8**: 629706.
- Perret, S.R., Thanawong, K., Basset-Mens, C., Mungkung, R.** 2013 The environmental impacts of lowland paddy rice: A case study comparison between rainfed and irrigated rice in Thailand. *Cah. Agric.* **22**(5): 369–377.
- Porazinska, D.L., Giblin-Davis, R.M., Faller, L., Farmerie, W., Kanzaki, N., Morris, K., Powers, T.O., Tucker, A.E., Sung, W., Thomas, W.K.** 2009 Evaluating high-throughput sequencing as a method for metagenomic analysis of nematode diversity. *Mol. Ecol. Resour.* **9**(6): 1439–1450.
- Ryss, A.Y.** 2017 A simple express technique to process nematodes for collection slide mounts. *J. Nematol.* **49**(1): 27–32.



- Sánchez-Moreno, S., Cano, M., López-Pérez, A., Benayas, J.M.R.** 2018 Microfaunal soil food webs in Mediterranean semi-arid agroecosystems. Does organic management improve soil health? *Appl. Soil Ecol.* **125**: 138–147.
- Schenk, J., Kleinbölting, N., Traunspurger, W.** 2019 Comparison of morphological, DNA barcoding, and metabarcoding characterizations of freshwater nematode communities. *Ecol. Evol.* **10(6)**: 2885–2899.
- Shafiqat, S., Bilgrami, A.L., Jairajpuri, M.S.** 1987 Evaluation of the predatory behaviour of *Dorylaimus stagnalis* Dujardin, 1845 (Nematoda: Dorylaimida). *Revue de Nématologie* **10**: 455–466.
- Sikder, M.M., Vestergård, M., Sapkota, R., Kyndt, T., Nicolaisen, M.** 2020 Evaluation of metabarcoding primers for analysis of soil nematode communities. *Diversity* **12(10)**: 388.
- Steel, H., Ferris, H.** 2016 Soil nematode assemblages indicate the potential for biological regulation of pest species. *Acta Oecol.* **73**: 87–96.
- Treonis, A.M., Unangst, S.K., Kepler, R.M., Buyer, J.S., Cavigelli, M.A., Mirsky, S.B., Maul, J.E.** 2018 Characterization of soil nematode communities in three cropping systems through morphological and DNA metabarcoding approaches. *Sci. Rep.* **8(1)**: 2004.
- Van Nguyen, S., Nguyen, P.T.K., Araki, M., Perry, R.N., Tran, L.B., Chau, K.M., Min, Y.Y., Toyota, K.** 2020 Effects of cropping systems and soil amendments on nematode community and its relationship with soil physicochemical properties in a paddy rice field in the Vietnamese Mekong Delta. *Appl. Soil Ecol.* **156**: 103683.
- Waeyenberge, L., de Sutter, N., Viaene, N., Haegeman, A.** 2019 New insights into nematode DNA-metabarcoding as revealed by the characterization of artificial and spiked nematode communities. *Diversity* **11(4)**: 52.
- Watanabe, T.** 2018 Paddy fields as artificial and temporal wetland. *Irrigation in Agroecosystems*, Gabor Ondrašek, IntechOpen.
- Win, P.P., Kyi, P.P., Maung, Z.T.Z., De Waele, D.** 2013 Population dynamics of *Meloidogyne graminicola* and *Hirschmanniella oryzae* in a double rice-cropping sequence in the lowlands of Myanmar. *Nematology* **15(7)**: 795–807.
- Yang, B., Chen, Q., Liu, X., Chen, F., Liang, Y., Qiang, W., He, L., Ge, F.** 2020 Effects of pest management practices on soil nematode abundance, diversity, metabolic footprint and community composition under paddy rice fields. *Front. Plant Sci.* **11**: 88.
- Yeates, G.W., Bongers, T., de Goede, R.G.M., Freckman, D.W., Georgieva, S.S.** 1993 Feeding habits in soil nematode families and genera—An outline for soil ecologists. *J. Nematol.* **25**: 315–331.
- Yin, W.** 1992 Pictorial keys to soil animals of subtropical China. Sciences press, Beijing, China. 618pp. [in Chinese]
- Yin, W.** 1998 Pictorial keys to soil animals of China. Sciences press, Beijing, China. 757pp. [in Chinese]
- Zhang, Z.Y., Zhang, X.K., Jhao, J.S., Zhang, X.P., Liang, W.J.** 2015 Tillage and rotation effects on community composition and metabolic footprints of soil nematodes in a black soil. *Eur. J. Soil Biol.* **66**: 40–48.
- Zheng, F., Zhu, D., Giles, M., Daniell, T., Neilson, R., Zhu, Y.G., Yang, X.R.** 2019 Mineral and organic fertilization alters the microbiome of a soil nematode *Dorylaimus stagnalis* and its resistome. *Sci. Total Environ.* **680**: 70–78.

Supplementary

Table S1. Total number of nematodes adopted for identification and the properties of individuals identified to the lowest taxonomic level

year	number	properties of individuals identified (%)			
		Genus	Family	Order	unidentified
2018	6839	98.06	1.26	0.13	0.56
2019	7536	91.85	0.13	1.74	6.28
2020	13676	95.57	1.57	1.53	1.33
Total	28051	95.18	1.11	1.24	2.47